JOURNAL OF SOLID STATE CHEMISTRY 40, 290–300 (1981)

The Six-Layer Structure of $BaSn_{0.9}Fe_{5.47}O_{11}$

M. C. CADÉE AND D. J. W. IJDO

Section of Solid State Chemistry, Gorlaeus Laboratories, Leiden State University, P.O. Box 9502, 2300 RA Leiden, The Netherlands

Received May 26, 1981; in final form August 4, 1981

The crystal structure of $BaSn_{0.9}Fe_{5.47}O_{11}$ was determined using neutron powder diffraction data and the profile refinement method. The hexagonal compound, space group $P\bar{3}m1$, has *hcc*-stacked BaO_3 and O_4 layers. A new building unit for this type of structure is introduced, the Q block with formula $Ba_2M_7O_{14}$, consisting of two *c*-stacked BaO_3 layers and two O_4 layers. Between the BaO_3 and O_4 layers one tetrahedral and one octahedral site is occupied; between the BaO_3 layers there are no other cations. $BaSn_{0.9}Fe_{5.47}O_{11}$ shows a magnetic behavior with an ordering temperature T_c of 420 K. Starting models for the structure determination were derived from the known structures of hexagonal ferrites and related compounds. Several isomorphs with formula $Ba_2Sn_2M^{2+}Fe_{10}O_{22}$ could be prepared, in which a partial substitution of Fe by Ga is possible. The nonstoichiometry of $BaSn_{0.9}Fe_{5.47}O_{11}$ can be explained by the surplus of positive charge if the available tetrahedral and octahedral sites of the structure are completely occupied with Sn^{4+} and Fe^{3+}. To achieve charge compensation either the occupation rates of Sn^{4+} and Fe^{3+} have to be lowered or a divalent ion has to be introduced, as is effected in the isomorphs.

Introduction

The compound $BaSn_{0.9}Fe_{5.47}O_{11}$ has been found in the $BaO–SnO_2–Fe_2O_3$ system (*1*). The reported unit cell parameters of this hexagonal compound, $a = 5.9367$, $c = 14.3364$ Å, suggest a structure comparable with $BaTi_2Fe_4O_{11}$ (*2*), which consists of a close-packed stacking of BaO_3 and O_4 layers. Structures of this type belong to an interesting group, including the hexagonal ferrites $BaFe_{12}O_{19}$ (*M*), $Ba_2Zn_2Fe_{12}O_{22}$ (*Y*), $Ba_2Fe_2^{2+}Fe_{28}^{3+}O_{46}$ (*X*), $BaFe^{2+}Fe_{16}^{3+}O_{27}$ (*W*) (*3*), and combinations of these structures (*4*). Furthermore, the spinel and perovskite structure and also the structure of $Ba_2Cr_{6.5}O_{14}$ (*5*) can be placed in this group. Usually, drawing only the (110) planes of the hexagonal structures of this group is sufficient to gain a good view of the complete structure (*3*).

Because single crystals of $BaSn_{0.9}Fe_{5.47}O_{11}$ could not be prepared, it was decided to determine the structure using the neutron powder profile refinement technique (*6*). This is a useful technique if models for the structure are available. Such models were derived from the known structures consisting of a close-packed stacking of BaO_3 and O_4 layers.

Experimental and Data Collecting

A 40-g sample of $BaSn_{0.9}Fe_{5.47}O_{11}$ was prepared by mixing appropriate ratios of $BaCO_3$, SnO_2, and Fe_2O_3 in a ball-mixer for a few hours and heating the mixture for a few hours at 1473 K. The reaction mixture

0022-4596/81/150290-11$02.00/0

was ground and heated for 1 day at 1473 K. After repeated grinding and heating with increasing heating times, a reaction mixture consisting of one phase, $BaSn_{0.9}Fe_{5.47}O_{11}$, according to the X-ray powder diffraction pattern, was obtained.

In view of the magnetic properties of this compound (see below), the neutron diffraction data were collected at 573 K, with the powder diffractometer of the Petten (The Netherlands) high-flux reactor. A wavelength of 2.5863(3) Å from the (111) planes of a copper monochromator was used with a 10′ collimation. The angular range $5.4° < 2\theta < 138.6°$ was scanned in steps of 0.072°. Absorption and extinction effects were small and no corrections were made. It was decided to correct for a probable preferred orientation with aid of the computer program and not to try to prepare a randomly oriented sample using glue, since its hydrogen content would cause a considerable background in the diffraction pattern.

Magnetic Properties

$BaSn_{0.9}Fe_{5.47}O_{11}$ shows a magnetic behavior with an ordering temperature T_c. This temperature was determined by measuring the magnetization with a field of about 1 kOe as a function of the temperature in high-temperature Faraday equipment. Details of this apparatus have been described elsewhere (*7*). Because our interest concerned only the T_c, the magnetization was measured in arbitrary units. By averaging the T_c's determined with increasing and decreasing temperature from the obtained plot of M versus T (Fig. 1), T_c was found to be 420(5) K. The increase of the magnetization with increasing temperature below T_c is caused by a strong magnetic anisotropy, which decreases with increasing temperature, facilitating magnetization at higher temperatures.

Experiments with a magnetically oriented powder sample (*8*) showed that the easy direction was neither along the 00l direction nor did it lie in the (00l) plane. The 110 reflection had increased in relative intensity, showing that the easy direction makes a small angle with the (00l) plane. The compound exhibits no retained magnetism. This was also observed in the magnetization curve at 4.2 K (Fig. 2) applying fields up to 56 kOe, using a PAR vibrating sample magnetometer (*9*). The compound was not saturated at the maximum field. Neutron powder diffraction at 300 K made it clear that the magnetic unit cell has the same a axis and a c axis of twice the nuclear c axis. The occurrence of magnetic 00l reflections in the diffraction pattern also shows the easy direction to have a component perpendicular to the 00l direction.

Models

According to the unit cell parameters, $BaSn_{0.9}Fe_{5.47}O_{11}$ has a six-layer structure of BaO_3 and O_4 layers. Consequently, there are 24 large atoms, viz. 2 Ba atoms and 22 O atoms or two BaO_3 and four O_4 layers. For such a six-layer structure a considerable number of models can be constructed. From the known structures consisting of a close-packed stacking of BaO_3 and O_4 layers some rules can be observed. The following rules were applied in reducing the number of possible models:

(a) Between two O_4 layers either three octahedral sites or one octahedral and two tetrahedral sites are occupied, these two ways of occupation usually alternating if a sequence of more than two O_4 layers occurs. In this way a tetrahedral coordination of the O atom is created, e.g., the spinel structure (*3*). This rule is valid only if the mean cation charge is considerably more than 2, as in the rocksalt structure, where between the two O_4 layers four octahedral sites are occupied, and in the zincite structure there are four tetrahedral sites. Three of the four tetrahedral sites being occupied,

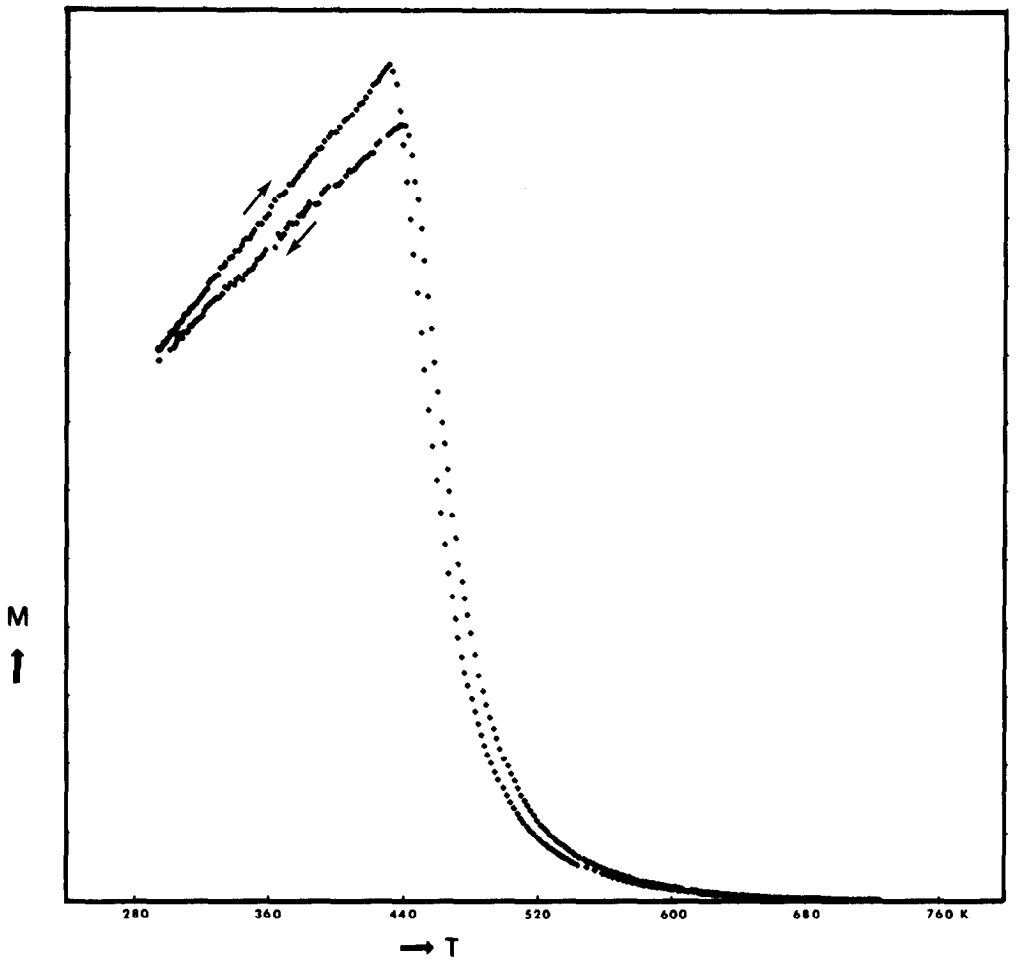

FIG. 1. Magnetization (M) of $BaSn_{0.9}Fe_{5.47}O_{11}$ in arbitrary units versus temperature (T) in K. The applied field was about 1 kOe.

a tetrahedral coordination of the O atom is reached only if between the adjacent O_4 layers three tetrahedral sites are likewise occupied.

(b) Between two BaO_3 layers only one octahedral site can be occupied, e.g., the structures of $BaTiO_3$ (*10*).

(c) Between a BaO_3 layer and an O_4 layer only one octahedral and one tetrahedral site can be occupied.

This means that a single hexagonal-stacked BaO_3 layer yields two occupied octahedral sites and one tetrahedral site with its bounding O_4 layers, for only one of the two face-sharing tetrahedral sites can be occupied. This situation is realized in $BaFe_{12}O_{19}$ and $BaTi_2Fe_4O_{11}$, in the so-called R-block (*2, 8*). A cubic-stacked single BaO_3 layer results in either two octahedral or two tetrahedral sites with the bounding O_4 layers. Combination of an occupied octahedral and tetrahedral site would, in this case, result in face-sharing of an octahedron and a tetrahedron, which is unlikely.

The occupation of the four available tetrahedral sites between a BaO_3 and an O_4

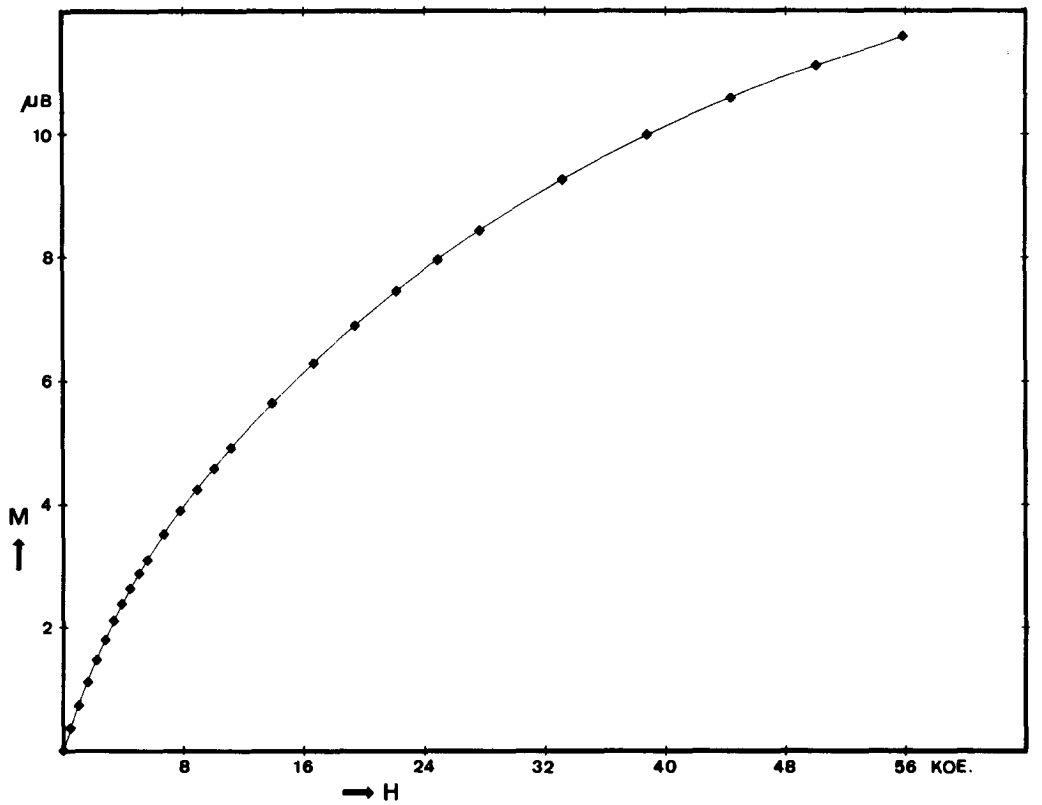

FIG. 2. Magnetization (M) of $BaSn_{0.9}Fe_{5.47}O_{11}$ in μ_B per unit cell versus the magnetic field (H) in kOe at 4.2 K.

layer results in edge-sharing tetrahedra and is therefore unlikely; for the reasons given under (a), occupation of three of the four tetrahedral sites being also unlikely.

For a six-layer sequence there are four possible ways of stacking, *c*, *h*, *hcc* and *hhhchc*, adopting the notation of Wells (*11*). In $BaSn_{0.9}Fe_{5.47}O_{11}$ there are 12.74 cations available to occupy tetrahedral and octahedral sites. Consequently, the models must possess at least 13 filled tetrahedral and octahedral sites. A six-layer model with two single BaO_3 layers yields a maximum of 12 filled tetrahedral and octahedral sites if the BaO_3 layers are *h*-stacked. This is realized in $BaTi_2Fe_4O_{11}$ (*2*).

For models with more than 12 sites to occupy, the only possibility is to join the two BaO_3 layers, leaving now three stacking possibilities:

h-Stacking of the BaO_3 layers yields three octahedral and two tetrahedral sites with the bounding O_4-layers. This is realized in the so called T-block (*8*), part of the structure of $Ba_2Zn_2Fe_{12}O_{22}$ (*Y*) (*3*).

c-Stacking of the BaO_3 layers; either three octahedral or two octahedral and two tetrahedral sites are available, the latter case being realized in $Ba_2Cr_{6.5}O_{14}$ (*5*). In this model there is no filled octahedral site between the two BaO_3 layers as there is with the T-block. We will call this the Q-block.

hc-Stacking of the BaO_3-layers; either

three octahedral and one tetrahedral or two octahedral and two tetrahedral sites are available.

The number of available models has been diminished further by applying Pauling's fifth rule, the rule of parsimony (*12*). This rule was found to be useful in the derivation of crystal structures (*13*). Models with low symmetry and consequently a large number of crystallographic positions as in the *hhhchc* stacked and in the *hcc*-stacked models with the BaO_3 layers *hc*-stacked have been rejected by applying this rule. The remaining models have been used as trial models for the profile refinement. These models are listed below and their atomic parameters are presented in Table I.

Model 1: cubic close-packed stacking, with, consequently, the Q-block. The cation arrangement between the O_4 layers is identical with the arrangement of the spinel structure, this model thus consisting of the Q-block and a spinel-block (Fig. 3a). This model has four tetrahedral and nine octahedral sites to occupy.

Model 2: hexagonal close-packed stacking, with consequently, the hexagonal-stacked T-block. The cation arrangement between the O_4 layers is as with the olivine structure (*14*). The connection between the T-block and the olivine structure is realized in such a way that between the first O_4 layers bounding to the T-block, three octahedral sites are filled. If two tetrahedral and one octahedral site were filled, a chain of five face-sharing octahedra would be obtained, which is unlikely. The resulting model has four tetrahedral and ten octahedral sites to occupy (Fig. 3b).

Model 3: *hcc* close-packed stacking, with the BaO_3-layers both *c*-stacked, which results in the Q-block and a spinel-block. The connection between these blocks is constructed such that the filled tetrahedral and octahedral site between the BaO_3 and the O_4 layer form a continuation of the spinel-block. This model has four tetrahedral and nine octahedral sites to occupy (Fig. 3c).

Models derived from the models 1 and 3, with a different cation distribution, i.e., two tetrahedral and one octahedral site between the O_4 layers bounding to the Q-blocks, result in a face-sharing tetrahedron and octahedron for the cubic stacking and in two face-sharing octahedra for the *hcc* stacking.

TABLE I

ATOMIC PARAMETERS OF THE TRIAL MODELS OF $BaSn_{0.9}Fe_{5.47}O_{11}$

Model	Space group	Ba	Oc(1)	Oc(2)	Oc(3)	Tetr(1)	Tetr(2)	O(1)	O(2)	O(3)	O(4)	O(5)	Position
		2*d*	1*a*	2*d*	6*i*	2*c*	2*d*	2*c*	2*d*	6*i*	6*i*	6*i*	
1	$P\bar{3}m1$	$\frac{1}{3}$	0	$\frac{1}{3}$	$\frac{1}{6}$	0	$\frac{1}{3}$	0	$\frac{1}{3}$	$\frac{1}{6}$	$\frac{1}{2}$	$\frac{1}{6}$	*x*
		$\frac{2}{3}$	0	$\frac{2}{3}$	$\frac{1}{3}$	0	$\frac{2}{3}$	0	$\frac{2}{3}$	$\frac{1}{3}$	1	$\frac{1}{3}$	*y*
		$\frac{1}{12}$	0	$\frac{1}{4}$	$\frac{1}{8}$	$\frac{3}{8}$	$\frac{1}{12}$	$\frac{1}{4}$	$\frac{11}{12}$	$\frac{1}{12}$	$\frac{1}{4}$	$\frac{7}{12}$	*z*
		2*d*	2*c*	2*c*	6*i*	2*d*	2*d*	2*d*	2*d*	6*i*	6*i*	6*i*	
2	$P\bar{3}m1$	$\frac{1}{3}$	0	0	$\frac{1}{2}$	$\frac{1}{3}$	$\frac{1}{3}$	$\frac{1}{3}$	$\frac{1}{3}$	$\frac{1}{6}$	$\frac{1}{6}$	$\frac{1}{6}$	*x*
		$\frac{2}{3}$	0	0	1	$\frac{2}{3}$	$\frac{2}{3}$	$\frac{2}{3}$	$\frac{2}{3}$	$\frac{1}{3}$	$\frac{1}{3}$	$\frac{1}{3}$	*y*
		$\frac{1}{12}$	$\frac{1}{2}$	$\frac{1}{3}$	$\frac{1}{8}$	$\frac{5}{8}$	$\frac{23}{24}$	$\frac{1}{12}$	$\frac{3}{4}$	$\frac{11}{12}$	$\frac{1}{4}$	$\frac{7}{12}$	*z*
		2*d*	1*a*	2*d*	6*i*	2*c*	2*d*	2*c*	2*d*	6*i*	6*i*	6*i*	
3	$P\bar{3}m1$	$\frac{1}{3}$	0	$\frac{1}{3}$	$\frac{1}{6}$	0	$\frac{1}{3}$	0	$\frac{1}{3}$	$\frac{1}{6}$	$\frac{1}{2}$	$\frac{1}{6}$	*x*
		$\frac{2}{3}$	0	$\frac{2}{3}$	$\frac{1}{3}$	0	$\frac{2}{3}$	0	$\frac{2}{3}$	$\frac{1}{3}$	1	$\frac{1}{3}$	*y*
		$\frac{1}{12}$	0	$\frac{1}{3}$	$\frac{1}{8}$	$\frac{3}{8}$	$\frac{23}{24}$	$\frac{1}{4}$	$\frac{1}{12}$	$\frac{11}{12}$	$\frac{1}{4}$	$\frac{7}{12}$	*z*

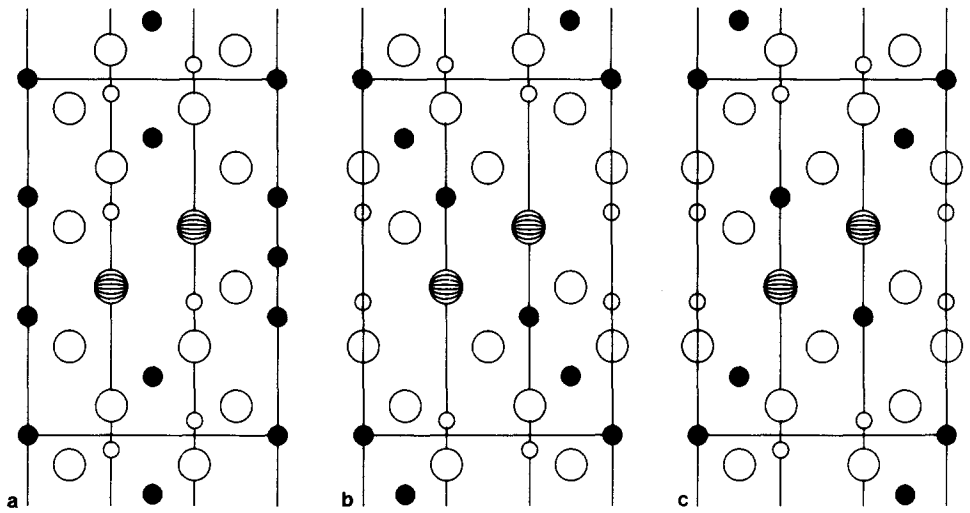

FIG. 3. The (110) planes of the trial models for the profile refinement of the neutron diffraction data: (a) Model 1, *h*-stacked; (b) Model 2, *c*-stacked; (c) Model 3, *hcc*-stacked. Shaded circles: Ba; open circles: O; small open circles: filled tetrahedral sites, solid circles: filled octahedral sites.

These models, though not very likely, were also tested in the profile refinement. They both generated high R values.

Structure Determination

The atomic parameters of the remaining models were used as starting parameters for the profile refinement (*6*). The variables in the first refinements were: a scale factor, three half-width parameters defining the Gaussian lineshape and the counter zero error. After the first runs the atomic position parameters, a preferred orientation parameter, and an asymmetry parameter below $2\theta = 40°$ were introduced. The use of a preferred orientation parameter is not surprising for hexagonal compounds, for the crystallites have a preference for a horizontal orientation of their (00l) planes. In the final stages of the refinement also the occupation rates of Fe and Sn in the octahedral sites are variable within the overall formula, because both Fe and Sn can occupy octahedral sites. The total occupation rate of a site could not exceed 100%, lower occupancies are possible because, according to the formula, not all the positions can be completely filled. The coherent scattering lengths assumed were: Ba—5.2, Sn—6.1, Fe—9.5, and O—5.8 fm (*15*). The Rietveld program minimizes the function:

$$X^2 = \sum_i w_i \left[y_i(\text{obs}) - \frac{1}{c} y_i(\text{calc}) \right]^2,$$

y(obs) and y(calc) represent the observed and calculated profile data point, w is the statistical weight allowed to each data point, and c the scale factor. The follow R factors are calculated:

$$R_{\text{nuclear}} = 100\, \Sigma \left| I_{(\text{obs})} - \frac{1}{c} I_{(\text{calc})} \right| \Big/ \Sigma I_{(\text{obs})});$$

$$R_{\text{profile}} = 100\, \Sigma \left| y_{(\text{obs})} - \frac{1}{c} y_{(\text{calc})} \right| \Big/ \Sigma y_{(\text{obs})});$$

$$R_{\text{weight}} = 100 \left[\left(\Sigma w \left| y_{(\text{obs})} - \frac{1}{c} y_{(\text{calc})} \right|^2 \Big/ \Sigma w \left| y_{(\text{obs})} \right|^2 \right]^{1/2}$$

$I_{(\text{obs})}$, $I_{(\text{calc})}$ = observed and calculated integrated intensity of each reflection.

For model 3, the following R factors were calculated: $R_{\text{nuclear}} = 5.05$, $R_{\text{profile}} = 11.70$,

TABLE II

ATOMIC POSITIONS, OCCUPATION RATES, AND CHARGE COMPENSATION OF THE O ATOMS IN THE STRUCTURE OF $BaSn_{0.9}Fe_{5.47}O_{11}$, SPACE GROUP $P\bar{3}m1$ (164)[a]

Atom	Position	x	y	z	Occupation rate (%)	Charge compensation
Ba	2*d*	0.3333	0.6667	0.425(2)	100	
Fe(1)	2*d*	0.3333	0.6667	0.955(1)	100	
Fe(2)	2*c*	0.0	0.0	0.378(1)	100	
Sn Fe Oc(1)	2*d*	0.3333	0.6667	0.680(1)	65(2) 35(2)	
Sn Fe Oc(2)	1*a*	0.0	0.0	0.0	50(4) 49(4)	
Fe Oc(3)	6*i*	0.170(1)	0.341(1)	0.173(1)	96(1)	
O(1)	2*c*	0.0	0.0	0.239(2)	100	2.19
O(2)	2*d*	0.3333	0.6667	0.087(2)	100	2.19
O(3)	6*i*	0.158(1)	0.316(2)	0.915(1)	100	2.19
O(4)	6*i*	0.486(1)	0.972(3)	0.247(1)	100	1.71
O(5)	6*i*	0.173(1)	0.346(2)	0.593(1)	100	1.86

[a] The SD_es of the last figure are included in parentheses.

R_{weight} = 13.44. The other models yielded high R factors. The final atomic parameters of model 3 are presented in Table II; Fig. 4 shows the agreement between the observed and calculated profiles, and Fig. 5 shows the (110) plane of the determined structure. The final overall isotropic temperature factor is found to be 0.87 Å². Also, the atomic isotropic temperature factors have been calculated, but gave slightly negative values for Fe(2) and O(1). Besides the R factors had not changed much. The relevant distances in the structure of $BaSn_{0.9}Fe_{5.47}O_{11}$ are reported in Table III, the relevant angles in Table IV.

Discussion

The occupation rates found for Sn and Fe in the octahedral sites of the structure investigated are less precise than the SDs given in Table II suggest. This is caused by the fact that an occupation of 50% Fe and 50% Sn at a certain position yields the same mean coherent scattering length as the occupation of only 82.2% Fe. Thus it is always possible to replace Sn by Fe and some vacancy. Nevertheless the observed preference of Sn for the Oc(1) position can be understood, since a better charge compensation of O(3), O(4), and O(5) is achieved by Sn on Oc(1) (Table II). For Oc(2) we found no preference for Fe or Sn and for Oc(3) a strong preference for Fe. The only way to attain further charge compensation is to move Fe from the tetrahedral to the

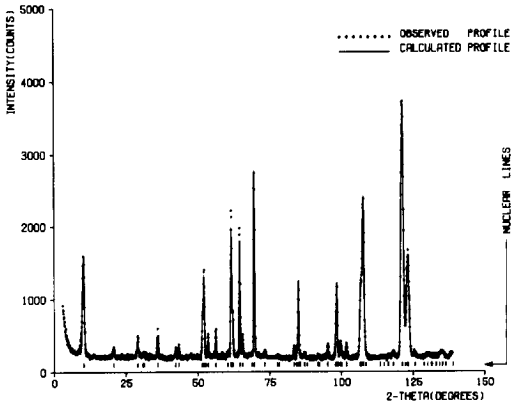

FIG. 4. The observed and calculated neutron diffraction profile of $BaSn_{0.9}Fe_{5.47}O_{11}$.

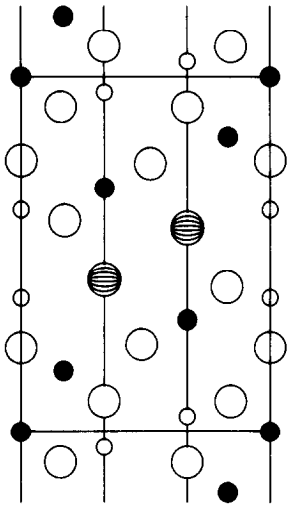

FIG. 5. The (110) plane of the found structure of $BaSn_{0.9}Fe_{5.47}O_{11}$.

octahedral sites. From the point of charge compensation it is not desirable to place Sn on the tetrahedral sites; moreover, Sn is never found to have a four coordination of oxygen. The removal of Fe from the tetrahedral to the octahedral sites did not result in a decrease of the *R* factors.

The Oc(1) octahedron is somewhat larger than the Oc(2) and Oc(3) octahedra, probably due to the Sn preference for Oc(1). The

TABLE III

RELEVANT DISTANCES IN THE STRUCTURE OF $BaSn_{0.9}Fe_{5.47}O_{11}$ IN Å

Attractive			Repulsive (below 3Å)		
Ba –O(4)	3.00(2)	3x	Oc(3)–Oc(3)	2.90(1)	3x
Ba –O(5)	2.92(2)	3x	O(1) –O(3)	2.74(2)	3x
Ba –O(5)	2.98(1)	6x	O(1) –O(4)	2.97(1)	6x
Oc(1)–O(4)	2.13(2)	3x	O(1) –O(5)	2.99(2)	3x
Oc(1)–O(5)	2.07(1)	3x	O(2) –O(3)	2.97(1)	6x
Oc(2)–O(3)	2.03(1)	6x	O(2) –O(4)	2.78(2)	3x
Oc(3)–O(1)	1.99(1)	1x	O(3) –O(3)	2.81(2)	2x
Oc(3)–O(2)	2.08(1)	1x	O(3) –O(4)	2.96(2)	2x
Oc(3)–O(3)	2.11(1)	2x	O(4) –O(4)	2.72(2)	2x
Oc(3)–O(4)	1.94(1)	2x	O(4) –O(5)	2.89(2)	2x
Fe(1)–O(2)	1.90(2)	1x	O(5) –O(5)	2.86(2)	2x
Fe(1)–O(3)	1.89(1)	3x			
Fe(2)–O(1)	1.99(2)	1x			
Fe(2)–O(5)	1.83(1)	3x			

TABLE IV

RELEVANT ANGLES (°) IN THE STRUCTURE OF $BaSn_{0.9}Fe_{5.47}O_{11}$

O(4)–Ba–O(4)	53.8(6)	3x	O(4)–Oc(1)–O(4)	97.8(6)	3x
O(4)–Ba–O(5)	177.1(6)	3x	O(4)–Oc(1)–O(5)	87.1(4)	6x
O(4)–Ba–O(5)	123.7(3)	6x	O(4)–Oc(1)–O(5)	172.5(8)	3x
O(4)–Ba–O(5)	86.3(5)	6x	O(5)–Oc(1)–O(5)	87.5(6)	3x
O(4)–Ba–O(5)	111.7(7)	6x	O(3)–Oc(2)–O(3)	87.7(4)	6x
O(4)–Ba–O(5)	57.9(4)	6x	O(3)–Oc(2)–O(3)	92.3(4)	6x
O(5)–Ba–O(5)	58.6(5)	3x	O(3)–Oc(2)–O(3)	180.0(0)	3x
O(5)–Ba–O(5)	57.3(4)	3x	O(1)–Oc(3)–O(2)	172.2(8)	1x
O(5)–Ba–O(5)	62.2(4)	3x	O(1)–Oc(3)–O(3)	83.9(6)	2x
O(5)–Ba–O(5)	65.9(4)	6x	O(1)–Oc(3)–O(4)	98.2(6)	2x
O(5)–Ba–O(5)	93.5(4)	6x	O(2)–Oc(3)–O(3)	90.3(5)	2x
O(5)–Ba–O(5)	119.2(1)	6x	O(2)–Oc(3)–O(4)	87.3(6)	2x
O(5)–Ba–O(5)	124.5(6)	6x	O(3)–Oc(3)–O(3)	83.6(6)	1x
O(5)–Ba–O(5)	169.6(9)	3x	O(3)–Oc(3)–(4)	93.7(5)	2x
O(2)–Fe(1)–O(3)	107.4(5)	3x	O(3)–Oc(3)–O(4)	176.3(6)	2x
O(3)–Fe(1)–O(3)	111.5(4)	3x	O(4)–Oc(3)–O(4)	89.1(9)	1x
O(1)–Fe(2)–O(5)	103.1(5)	3x			
O(5)–Fe(2)–O(5)	115.1(3)	3x			

Sn^{4+} radius in a six-coordination of oxygen is 0.690 Å and for Fe^{3+} (high spin) 0.645 Å (16). The mean cation–oxygen distance is 2.10 Å for Oc(1) and 2.03 Å for Oc(2) and Oc(3). The latter distance is in good agreement with that found in other compounds; e.g., the mean Fe–O distance in the octahedra of $BaFe_{12}O_{19}$ is 2.01 Å (17). The distortions of the octahedra in $BaSn_{0.9}Fe_{5.47}O_{11}$ are caused by Ba having a larger ionic radius (1.60 Å) than O (1.38 Å) (*16*). The mean Fe–O distance of the tetrahedral Fe(1) is 1.89 Å, and of the tetrahedral Fe(2) 1.87 Å, in good agreement with other ferrites, e.g., $BaCaFe_4O_8$ (*18*) and $BaSrFe_4O_8$ (*19*), both with a mean Fe–O distance of 1.86 Å. The considerable distortion of the tetrahedon of Fe(2) can be explained by the charge compensation, which is low for O(5) and high for O(1), resulting in a short Fe(2)–O(5) and a larger Fe(2)–O(1) distance. For the tetrahedron of Fe(1), the O atoms have an almost equal charge compensation, and consequently this tetrahedon is almost ideal.

The Ba atom is found to have a 12-coordination of O atoms with a mean Ba–O distance of 2.97 Å. In $Ba_2Zn_2Fe_{12}O_{22}$ (Zn_2Y), the mean Ba–O distance is 2.985 Å (*20*). All oxygen atoms have a four-coordi-

nation, except O(5) which is coordinated by five cations. The O_4 layers at $z = \pm 1/12$ are slightly nonplanar (0.03 Å), at $z = \pm\frac{1}{4}$ the separation is 0.11 Å and in the BaO_3 layers this separation has increased to 0.25 Å. In the T-block of $Ba_2Zn_2Fe_{12}O_{22}$ (Zn_2Y) this separation is 0.20 Å (*20*).

The structure of $BaSn_{0.9}Fe_{5.47}O_{11}$ reported here introduces a new building unit in the structures of hexagonal ferrites and related compounds, the Q-block. This Q-block, the (110) plane of which is depicted in Fig. 6, consists of a pair of cubic stacked BaO_3 layers with at either side an O_4 layer that is usually hexagonal stacked. There are no cations between the two BaO_3 layers and between the BaO_3 and the O_4 layer one tetrahedal and one octahedral site is occupied. The Q-block is comparable with the completely hexagonal stacked T-block (8), but has one octahedral site less to fill. The remarkable three face-sharing octahedra in the T-block are avoided here because the BaO_3 layers are *c*-stacked. The structure of $BaSn_{0.9}Fe_{5.47}O_{11}$ can be described as QS, where S means the spinel-block (*8*). The comparable structure with the T-block, $(TS)_3$ is realized in $Ba_2Zn_2Fe_{12}O_{22}$ (Zn_2Y). The structure of $Ba_2Cr_{6.4}O_{14}$ (*5*) can be described as $(Q)_3$, the (110) plane of this structure is depicted in Fig. 7. A structure consisting of only T-blocks has not been reported in the literature. Despite the long superexchange path between the Fe(2) atoms at either side of the pair of BaO_3 layers, the magnetic ordering temperature of $BaSn_{0.9}Fe_{5.57}O_{11}$ is relatively high. A similar long superexchange path is found in the antiferromagnetic compounds $BaCaFe_4O_8$ (*18*) and $BaSrFe_4O_8$ (*19*), where high Néel temperatures are also observed.

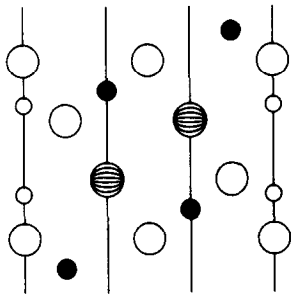

FIG. 6. The (110) plane of the Q block, the introduced new building unit in hexagonal ferrites and comparable structures.

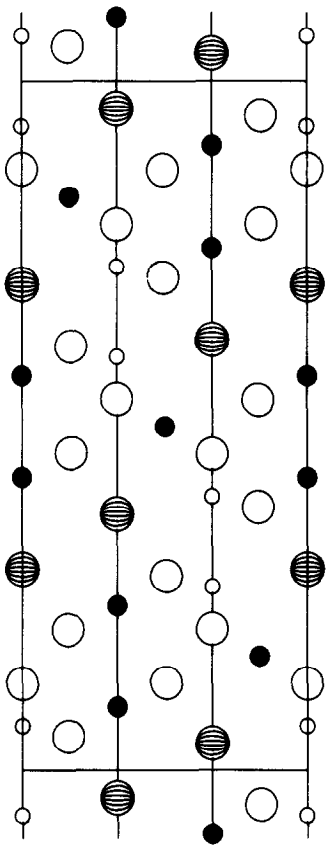

FIG. 7. The (110) plane of the structure of $Ba_2Cr_{6.5}O_{14}$ $(Q)_3$ after Evans and Katz, 1972. The tetrahedral sites are partly filled by Cr^{6+} and the octahedral sites are completely filled by Cr^{3+}. All (110) planes were generated using the crystallographic plotting program FIGATOM (*21*).

Isomorphs

As pointed out above the structure of $BaSn_{0.9}Fe_{5.47}O_{11}$ possesses four tetrahedral and nine octahedral sites. If a divalent ion is

introduced it is possible to fill all these sites completely. With one divalent ion in the unit cell this leads to the formula $Ba_2Sn_2M^{2+}Fe_{10}O_{22}$. It was possible to synthesize compounds of this type with M^{2+} = Mg, Mn, Co, Ni, and Zn by a solid-state reaction at 1473 K (see above); for Cu and Cd the reactions were carried out at 1323 K, because the Cu containing mixture partly melted at 1473 K and CdO is volatile at this temperature. The M^{2+} ion was introduced as the monoxide for Co, Cu, Zn, and Cd. Mn was introduced as MnO_2, but at 1473 K Mn^{4+} rapidly reduces to Mn^{2+} if these divalent ions can be incorporated in the structure. Mg and Co were introduced as carbonates. No attempt was made to apply Fe^{2+} because of expected difficulties on account of the oxygen pressure. A partial substitution of Fe by Ga can also be effected, Ga being introduced as Ga_2O_3. The unit cell parameters and the available magnetic ordering temperatures of these compounds are presented in Table V.

TABLE V

UNIT CELL PARAMETERS AT 295 K AND THE AVAILABLE MAGNETIC ORDERING TEMPERATURES T_c OF THE ISOMORPHS OF $BaSn_{0.9}Fe_{5.47}O_{11}$

Compound	a (Å)	c (Å)	T_c (K)
$BaSn_{0.9}Fe_{5.47}O_{11}$	5.923(1)	14.291(1)	420(5)
$BaSn_{0.9}GaFe_{4.47}O_{11}$	5.909(1)	14.313(2)	
$Ba_2Sn_2MgFe_{10}O_{22}$	5.930(1)	14.314(1)	334(5)
$Ba_2Sn_2MnFe_{10}O_{22}$	5.943(1)	14.334(2)	380(5)
$Ba_2Sn_2MnGa_2Fe_6O_{22}$	5.92891)	14.346(2)	
$Ba_2Sn_2CoFe_{10}O_{22}$	5.929(1)	14.318(2)	378(5)
$Ba_2Sn_2NiFe_{10}O_{22}$	5.921(1)	14.296(1)	444(5)
$Ba_2SnNiGa_2Fe_6O_{22}$	5.902(1)	14.301(2)	
$Ba_2Sn_2NiGa_4Fe_6O_{22}$	5.895(1)	14.299(2)	
$Ba_2Sn_2CuFe_{10}O_{22}$	5.925(1)	14.303(2)	375(5)
$Ba_2Sn_2CuGa_2Fe_8O_{22}$	5.921(1)	14.342(3)	
$Ba_2Sn_2ZnFe_{10}O_{22}$	5.933(1)	14.329(2)	
$Ba_2Sn_2ZnGa_2Fe_8O_{22}$	5.917(1)	14.335(2)	
$Ba_2Sn_2ZnGa_3Fe_7O_{22}$	5.913(1)	14.333(3)	
$Ba_2Sn_2CdFe_{10}O_{22}$	5.954(1)	14.365(2)	
$Ba_2Sn_2CdGa_2Fe_8O_{22}$	5.940(1)	14.383(2)	

The existence of isomorphous compounds with a divalent ion and completely filled octahedral and tetrahedral sites implies that the lack of divalent ions in the reaction mixture is responsible for the nonstoichiometry of $BaSn_{0.9}Fe_{5.47}O_{11}$. There is simply a surplus of positive charge with the available tetrahedral and octahedral sites completely filled by Fe^{3+} and Sn^{4+}. Charge compensation then is achieved by lowering the occupation rates of Sn^{4+} with about 10% and Fe^{3+} with 1%. In this way the occupation rate remains almost as high as possible.

Attempts to synthesize some of the corresponding Ti, Ru, and Sr isomorphs met with no success. Compounds of the type $(QS_2)_3$ could not be prepared; in the literature, no evidence was found for the existence of compounds of the type TS_2. Neutron powder diffraction experiments will be carried out on $Ba_2Sn_2MnFe_{10}O_{22}$ in order to investigate the occupation of the tetrahedal and octahedral sites and to determine the magnetic structure. The magnetic properties of $BaSn_{0.9}Fe_{5.47}O_{11}$ and its isomorphs will be investigated in the near future.

Acknowledgments

We wish to thank Mr. J. F. Strang of the Energieonderzoek Centrum Nederland (ECN, Petten, The Netherlands) for collecting the neutron powder diffraction data, Dr. D. W. Engelfriet and Mr. B. v.d. Griendt for the magnetic measurements, Dr. G. H. Jonker for critically reading the manuscript, and Miss S. Amadio for reviewing the English manuscript.

References

1. M. C. CADÉE AND D. J. W. IJDO, *J. Solid State Chem.* **36**, 314 (1981).
2. F. HABEREY AND M. VELICESCU, *Acta Crystallogr. Sect. B* **30**, 1507 (1974).
3. P. B. BRAUN, *Philips Res. Rep.* **12**, 491 (1957).
4. J. S. ANDERSON AND J. L. HUTCHINSON, *Cont. Phys* **16**, 443 (1975).
5. D. M. EVANS AND L. KATZ, *Acta Crystallogr. Sec. B* **28**, 1219 (1972).

6. H. M. RIETVELD, *J. Appl. Cryst.* **2,** 65 (1969).
7. J. W. ARBOUW, Thesis, Universiteit Leiden (1974).
8. J. SMIT AND H. P. J. WIJN, "Ferrites." Eindhoven,(1959).
9. H. T. WITTEVEEN, Thesis, Universiteit Leiden (1973).
10. R. D. BURBANK AND H. T. EVANS, *Acta Crystallogr.* **1,** 330 (1948).
11. A. F. WELLS, "Structural Inorganic Chemistry," 4th ed., Oxford Univ. Press, London (1975).
12. L. PAULING, *J. Amer. Chem. Soc.* **51,** 1010 (1929).
13. A. B. A. SCHIPPERS, Thesis, Universiteit Leiden (1975).
14. R. W. G. WYCKHOFF, "Crystal Structures," 2nd ed. Interscience, New York (1965).
15. G. E. BACON, *Acta Crystallogr. Sect. A* **28,** 357 (1972).
16. R. D. SHANNON AND C. T. PREWITT, *Acta Crystallogr. Sect. B* **25,** 925 (1969).
17. W. D. TOWNES, J. H. FANG, AND A. J. PERROTTA, *Z. Kristallgr.* **125,** 437 (1967).
18. D. HERRMANN AND M. BACKMANN, *Mater. Res. Bull.* **6,** 725 (1971).
19. M. C. CADÉE, *Acta Crystallogr. Sect. B* 31, 2012 (1975).
20. W. D. TOWNES AND J. H. FANG, *Z. Kristallgr.* **131,** 196 (1970).
21. G. A. LANGLET, *J. Appl. Crystallogr.* **5,** 66 (1972).